Supplemental Information

PET data acquisition

After at least six hours fasting, participants received a bolus injection of 18FDG (approximately 200 MBq) in the antecubital fossa and were placed in a dedicated waiting room, where they were instructed to remain sitting quietly without reading or music, but eyes open, in accordance with a nominal resting state. After a 45-min uptake period, each person was positioned in the scanner (HR+ PET camera (CTI; Knoxville, TN)) and the head was aligned in the scanner relative to the canthomeatal line and gently fixated to minimize head movements. Sixty-three contiguous slices of 2.5 mm were acquired over approximately 20 min in 3D mode. Images were reconstructed using an iterative algorithm to an in-plane resolution of 4.5 mm. Photon attenuation measurements were made with rotating pin sources containing 68Ge. Additional corrections in the reconstruction process accounted for scattered radiation, random coincidences, and counting losses due to dead time in the camera electronics.

Skin conductance acquisition and analysis

No more than five days later, skin conductance data were obtained during fMRI scanning. A Coulbourn Modular Instruments System (Allentown, PA) was used to record skin conductance levels via a Coulbourn Isolated Skin Conductance Coupler (S71-23) using a constant 0.5 V through 8 mm (sensor diameter) Ag/AgCl radiotranslucent electrodes (BioPac Systems Inc., Goleta, CA). Electrodes were filled with isotonic paste and placed on the palm of the participant's left hand. The skin conductance electrodes were separated by 14 mm, as determined by the width of the adhesive collar. A Coulbourn Lablinc Analog-to-Digital Converter (V19-16)

digitized the analog signals, which were then sampled and stored by a PC. Skin conductance responses (SCRs) to the conditioned stimuli in the various experimental phases were calculated by subtracting the mean skin conductance level two seconds prior to the context presentation from the maximal skin conductance level during the cue presentation. To assess metabolic predictors of fear extinction, change in SCRs was calculated by subtracting SCRs to the last four previously reinforced cue presentations from SCRs to the first four previously reinforced cue presentations during the extinction phase. To calculate residual fear at the beginning of the extinction recall phase, difference in SCRs was calculated by taking SCRs to the first four extinguished cue presentations minus SCRs to adjacent non-reinforced cue presentations; the same calculations were performed for the first four unextinguished cue presentations. The difference of difference scores between the extinguished and unextinguished cue presentations were then entered into a linear regression model with the PET FDG data to compute correlations at each voxel.

MRI data acquisition

fMRI was performed with a Trio 3.0 Tesla whole-body, MRI system (Siemens Medical Systems, Iselin, New Jersey) equipped for echo planar imaging (EPI) with a 32-channel head coil. Subjects were instructed to lie as still as possible and head movement was restricted with foam cushions. After an automated scout image was obtained and automated shimming procedures were performed, a high-resolution structural scan was collected to facilitate spatial normalization and to position the subsequent scans. fMRI images, sensitive to blood oxygenation level dependent (BOLD) contrast, were acquired with a descending gradient echo T2*-weighted sequence (TR= 2560 ms, TE= 30ms, Flip angle = 90°), collected in 48 coronal oblique slices

tilted 38° down from the anterior-posterior commissure line. The voxel size was 3×3×2.5 mm with a 0.5 mm slice gap.

Exploratory "psychophysiological" interactions (PPI) analysis of the amygdala

An exploratory psychophysiological interaction (PPI) functional connectivity analysis was also performed on the extinction recall neuroimaging dataset with BOLD time course averaged across the left and right amygdala (Anatomical Automatic Labeling definition) as the seed variable. (Note here that the term "psychophysiological" does not refer to skin conductance but rather to within-fMRI BOLD associations.) The time course was hemodynamically deconvolved (1, 2), and the interaction between the first four extinguished and non-extinguished cue presentations on a voxelwise basis was calculated using the PPI function in SPM8. The PPI, the seed and the experimental regressors were entered in a first level model, along with six movement parameters. First level contrasts representing the PPI were entered in a second level one-sample t-test for amygdala seed. The resulting map represents areas that display increased or decreased functional connectivity to the amygdala dependent on the cue's having been previously extinguished or non-extinguished. A threshold of $p<0.001$ with cluster exceeding 10 voxels was chosen for these exploratory analyses.

Results indicate that for the left amygdala, the medial frontal gyrus, extending into the dorsal anterior cingulate, displayed an increased functional coupling to the amygdala when the extinguished cue was presented, as compared to the non-extinguished cue. The ventromedial prefrontal cortex displayed a decrease in functional coherence. The right amygdala displayed only minimal PPI effects; see Supplementary table 2 and Supplementary figure 5.

Although the directionality of the connectivity changes was somewhat counterintuitive, with lower amygdala-to-ventromedial-prefrontal-cortex connectivity during extinguished cue, the results largely support the functional involvement of the ventromedial prefrontal cortex and dorsal cingulate/medial frontal gyrus in extinction recall. Of note, the directionality of the findings are largely consistent with those observed in resting state connectivity analyses of the centromedial and basolateral amygdala (3).

Figure S1.

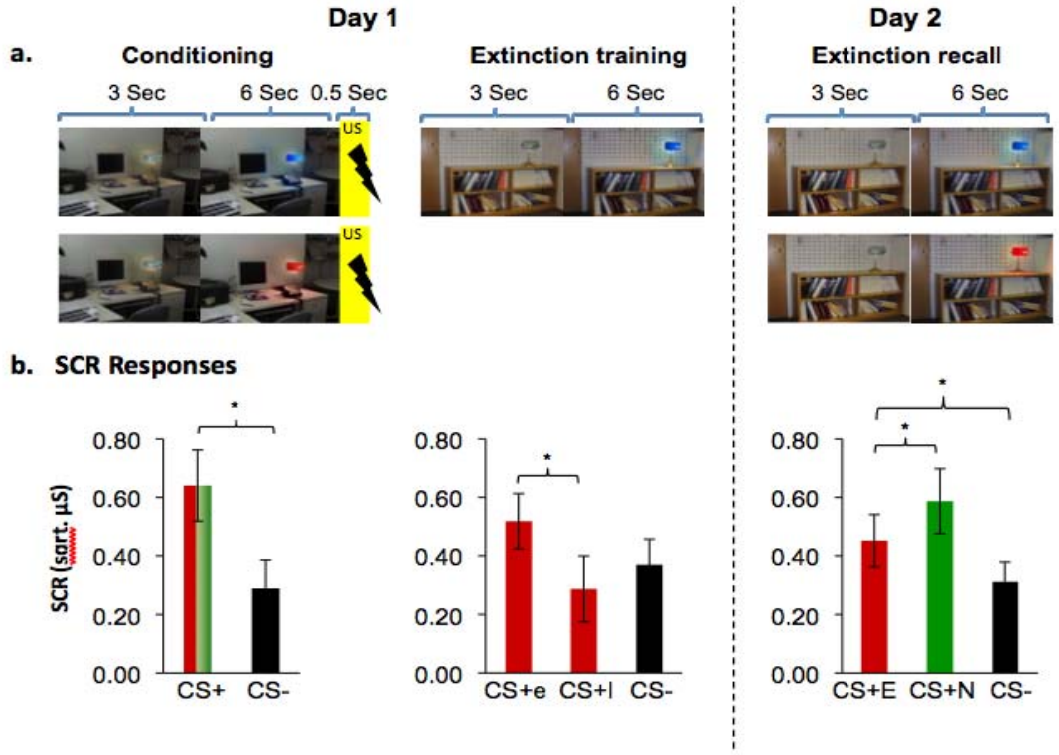

a) Stimuli presented during fear conditioning, extinction and subsequent recall (memory) of extinction. Two stimuli (e.g., a red and a blue light appearing in either a library or office context, termed the reinforced conditioned stimuli, or CS+'s) were paired with an electric shock unconditioned stimulus during the conditioning phase. Shortly thereafter, one of the CS+'s), e.g., the blue light, was extinguished. On the next day, the blue extinguished stimulus (CS+E), and the red non-extinguished stimulus (CS+N), were repeatedly presented to test for extinction memory. A yellow light (not shown) served as a non-reinforced conditioned stimulus (CS-). Colors were counterbalanced across subjects. b) Mean skin conductance responses (SCRs) to i) the CS+ trials during conditioning, ii) the subsequent early CS+E (CS+e) and the late CS+E (CS+l) extinction trials, and iii) the CS+E and CS+N trials during extinction recall the following day. Note that during fear conditioning, SCRs were elevated to the two CS+'s combined, compared to

the CS- (SCR difference = 0.35 $\mu S^{½}$, paired t(17) = 5.0, p < 0.001). Extinction training led to a diminution of SCRs to the CS+ (change in SCRs from early to late = 0.23 $\mu S^{½}$, paired t(17) = 2.0, p = 0.033). During the extinction recall test the next day, SCRs to CS+E were lower than to the CS+N (difference in SCRs = 0.13 $\mu S^{½}$, paired t(17) = 1.8, p = 0.046), indicating successful retention of the extinction memory . Due to the directionality of the predictions, all p values are one-tailed.

Figure S2.

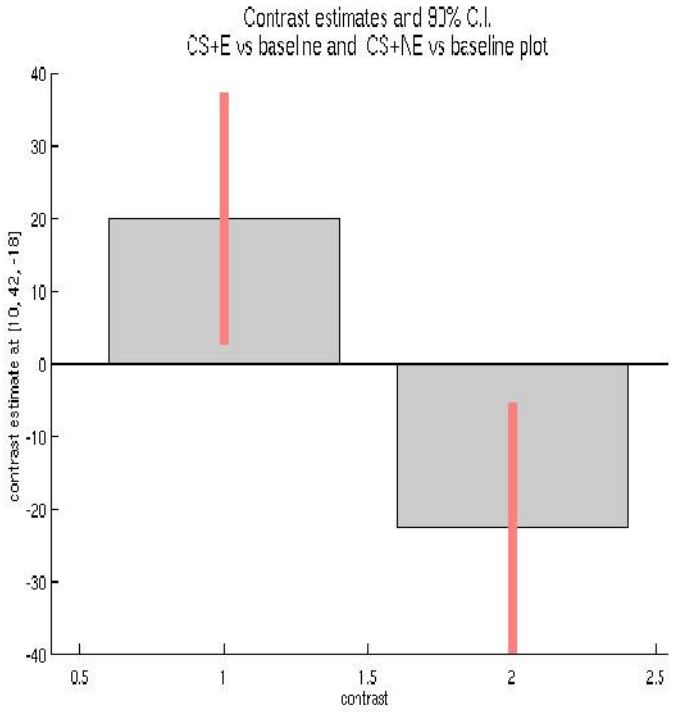

Ventromedial prefrontal cortex response at x=10, y= 42, z= -18 during presentation of the CS+E versus fixation baseline (left) and presentation of the CS+U versus fixation baseline (right), during extinction recall. The figure illustrates that the observed effect is driven by ventromedial prefrontal cortex activation to the CS+E and deactivation to the CS+N.

Figure S3

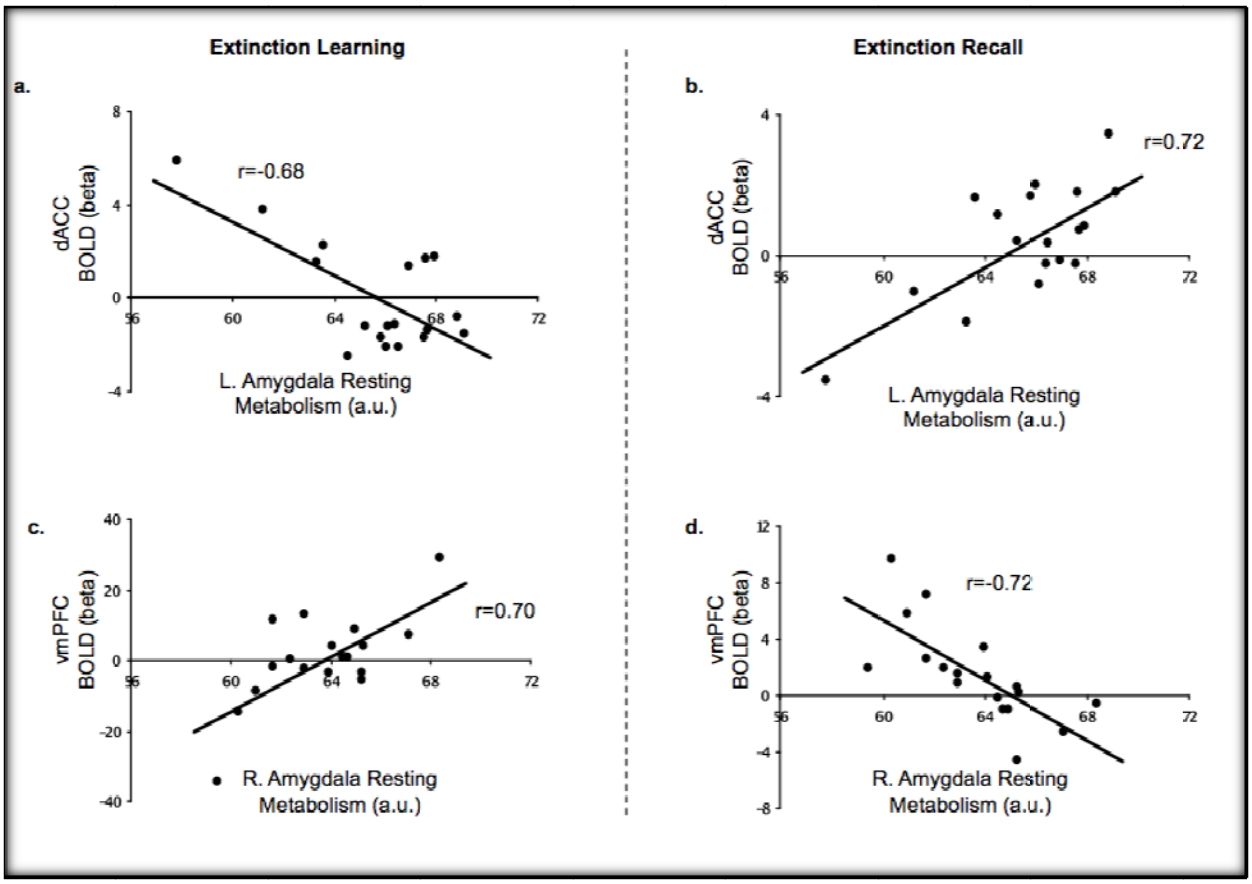

Scatter plots of BOLD parameter estimates and resting amygdala metabolism. Left amygdala metabolism negatively predicted dorsal anterior cingulate BOLD activation during extinction learning (a) and positively predicted dorsal anterior cingulate BOLD reactivity during extinction recall (b). Right amygdala metabolism positively predicted ventromedial prefrontal BOLD reactivity during extinction learning (c) and negatively predicted ventromedial prefrontal BOLD reactivity during extinction recall (d). a.u. = arbitrary units.

Figure S4

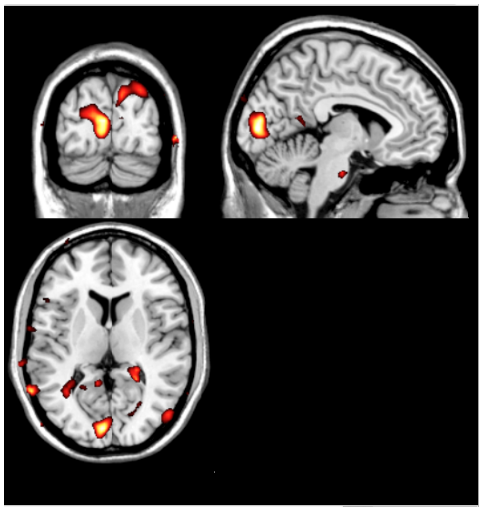

Intra-regional relationships in primary visual cortex (anatomical mask of Brodmann area 17). Resting metabolism was entered as a covariate in a linear regression model to predict BOLD activation to all visual stimuli compared to a non-visual baseline (presentation of a black screen). Primary visual cortex metabolism was found to predict its own functional reactivity to visual stimuli in this ROI-to-ROI analysis, $t=4.92$, $p<0.001$. Red areas indicate higher correlations between primary visual cortex metabolism and BOLD activation during visual stimuli. Results are illustrated with a threshold of $t\ (17) > \pm 2.5$ and overlaid on a template structural MR image.

Figure S5

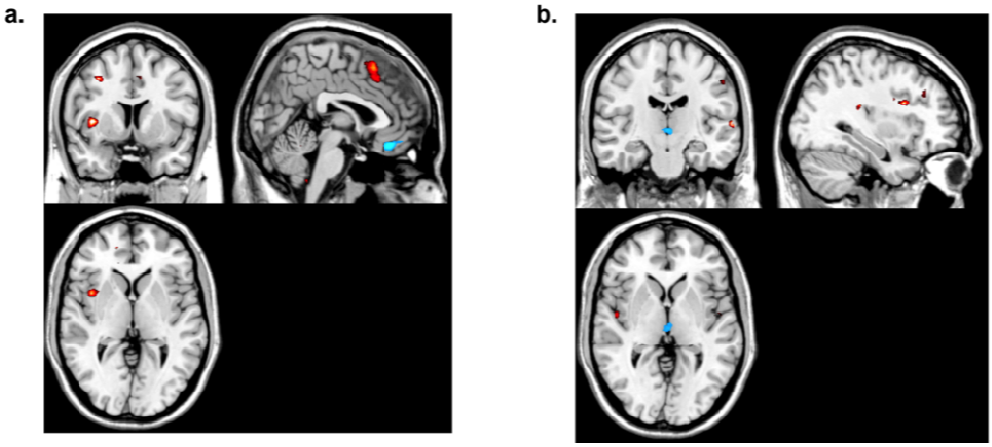

Results from a psychophysiological interaction (PPI) analysis of the amygdala during extinction recall. Left a) and right b) amygdala PPI effects. Red indicates higher, and blue lower, connectivity with the amygdala during presentations of the CS+N compared to the CS+E. Psychophysiological interactions are illustrated with a threshold of t (17) > ±3 and overlaid on a template structural MR image.

Supplementary Table 1. Whole brain results

Contrast

Early Extinction

First four CS+ > CS-

Cluster			Peak					
P_{FWE}	P_{FDR}	Size	P_{FWE}	P_{FDR}	T	Z	MNI $_{XYZ}$	Nearest gray matter
0.002	0.107	470	0.001	0.101	4.99	4.59	60 24 24	Right Inferior Frontal Gyrus
			0.174	0.13	4.81	4.44	60 22 32	Right Middle Frontal Gyrus
			0.947	0.5	3.86	3.66	50 14 44	Right Middle Frontal Gyrus

First four CS- > CS+

Cluster			Peak					
P_{FWE}	P_{FDR}	Size	P_{FWE}	P_{FDR}	T	Z	MNI $_{XYZ}$	Nearest gray matter
0.013	0.148	337	0.001	0.053	5.2	4.76	-16 -36 76	Left Postcentral Gyrus
				0.724	4.17	3.92	-10 -24 80	White matter
0	0.009	1110	0.08	0.103	5.07	4.65	38 -24 68	Right Precentral Gyrus
			0.236	0.183	4.7	4.36	54 -14 56	Right Postcentral Gyrus
			0.575	0.427	4.31	4.04	34 -32 64	Right Precentral Gyrus

Late Extinction

Last four CS+ > CS-
No significant clusters

Last four CS- > CS+
No significant clusters

Early versus late Extinction

First four CS+ > Last four CS+

Cluster	Peak

P_{FWE}	P_{FDR}	Size	P_{FWE}	P_{FDR}	T	Z	MNI $_{XYZ}$	Nearest gray matter
0.000	0.000	2217	0.001	0.014	6.42	5.65	62 20 32	Right Middle Frontal Gyrus
			0.029	0.041	5.39	4.9	42 26 8	Right Inferior Frontal Gyrus
			0.03	0.041	5.37	4.89	60 24 24	Right Inferior Frontal Gyrus
0.000	0.000	7944	0.006	0.034	5.86	5.25	-38 -70 -24	Left Cerebellum, Declive
			0.009	0.04	5.73	5.16	28 -96 4	Right Middle Occipital Gyrus
			0.012	0.041	5.66	5.1	38 -86 -8	Right Inferior Occipital Gyrus
0.000	0.000	1348	0.034	0.041	5.34	4.86	-50 16 44	Left Middle Frontal Gyrus
			0.142	0.061	4.88	4.5	-42 16 -2	Left Inferior Frontal Gyrus
			0.175	0.067	4.81	4.44	-50 18 14	Left Inferior Frontal Gyrus
0.000	0.000	1281	0.034	0.041	5.34	4.86	-36 -66 54	Left Superior Parietal Lobule
			0.087	0.059	5.04	4.63	-64 -54 38	Left Supramarginal Parietal Gyrus
			0.21	0.078	4.74	4.39	-42 -58 60	Left Inferior Parietal Lobule
0.000	0.000	733	0.049	0.045	5.23	4.77	-8 -4 4	Left Thalamus
			0.097	0.06	5.01	4.6	12 -2 4	Right Thalamus
			0.273	0.088	4.64	4.31	-6 -14 8	Left Thalamus
0.000	0.000	1013	0.089	0.059	5.03	4.62	34 -54 40	Right Inferior Parietal Lobule
			0.107	0.06	4.97	4.58	36 -64 52	Right Superior Parietal Lobule
			0.16	0.065	4.84	4.47	44 -62 48	Right Superior Parietal Lobule
0.008	0.004	368	0.089	0.059	5.03	4.62	4 -24 24	Right Cingulate Gyrus
			0.23	0.08	4.71	4.36	10 -16 30	Right Cingulate Gyrus
			0.315	0.097	4.59	4.27	-4 -26 26	Left Cingulate Gyrus

0.001	0.001	554	0.217	0.078	4.73	4.38	38 52 -8	Right Middle Frontal Gyrus
			0.526	0.155	4.36	4.08	26 54 -2	Right Superior Frontal Gyrus
			0.773	0.242	4.12	3.87	42 42 -18	Right Middle Frontal Gyrus
0.001	0.004	505	0.322	0.097	4.58	4.26	8 -66 44	Right precuneus
			0.346	0.101	4.55	4.23	12 -64 36	Right Precuneus
			0.739	0.224	4.15	3.9	-8 -70 48	Left Precuneus
0.000	0.000	687	0.338	0.1	4.56	4.24	-40 54 0	Left Middle Frontal Gyrus
			0.785	0.246	4.1	3.86	-44 46 14	Left Middle Frontal Gyrus
			0.822	0.269	4.06	3.83	-42 42 26	Left Middle Frontal Gyrus

Last four CS+ late > first four CS+

Cluster			Peak					
P_{FWE}	P_{FDR}	Size	P_{FWE}	P_{FDR}	T	Z	MNI $_{XYZ}$	Nearest Gray Matter
0.011	0.566	347	0.401	0.865	4.49	4.18	32 -18 50	Right Precentral Gyrus
			0.924	0.865	3.91	3.7	56 -12 54	Right Postcentral Gyrus
			0.983	0.865	3.73	3.55	32 -24 56	Right Precentral Gyrus

Recall

First four CS+ non extinguished > first four CS+ extinguished

Cluster			Peak					
P_{FWE}	P_{FDR}	Size	P_{FWE}	P_{FDR}	T	Z	MNI $_{XYZ}$	Nearest Gray Matter
0.009	0.026	318	0.459	0.495	4.24	4.15	38 8 14	Right Anterior Insula
		0.943	0.59	3.76	3.7	0.000	42 20 16	Right Inferior Frontal Gyrus
		0.948	0.59	3.75	3.69	0.000	34 30 18	Right Inferior Frontal Gyrus

First four CS+ extinguished > first four CS+ non-extinguished

No significant clusters

Metabolism to Extinction BOLD correlations

dACC metabolism positive correlates to extinction BOLD

Cluster			Peak					
P_{FWE}	P_{FDR}	Size	P_{FWE}	P_{FDR}	T	Z	MNI $_{XYZ}$	Nearest Gray Matter
0.007	0.025	253	0.091	0.278	7.59	4.88	62 -10 -30	Right Fusiform Gyrus
0.040	0.025	177	0.915	0.65	5.23	3.94	-50 -56 32	Left Supramaginal Gyrus
0.001	0.002	364	0.962	0.68	5.03	3.84	60 -50 30	Right Supramaginal Gyrus
			0.999	0.714	4.52	3.58	54 -42 42	Right Inferior Parietal Lobule
			0.999	0.714	4.48	3.55	46 -40 26	Right Posterior Insula

vmPFC/dACC metabolism negative correlates to extinction BOLD

Cluster			Peak					
P_{FWE}	P_{FDR}	Size	P_{FWE}	P_{FDR}	T	Z	MNI $_{XYZ}$	Nearest Gray Matter
0.006	0.017	258	0.394	0.783	6.37	4.43	-22 26 14	Left Claustrum
			0.437	0.783	6.27	4.39	-26 36 16	White matter
			0.742	0.985	5.66	4.13	-24 34 6	White matter

dACC metabolism displayed no significant negative correlates to extinction BOLD, vmPFC/dACC metabolism displayed no significant positive correlations to extinction BOLD, left and right amygdala, and vmPFC metabolism displayed no significant correlations to extinction.

There were no significant correlations to Recall BOLD signal in any contrasts outside the *a priori* regions.

Supplementary Table 2. Whole brain results

Psychophysiological interaction analyses

Left amygdala seed

Positive PPI's

Cluster			Peak				
P_{FWE}	P_{FDR}	Size	P_{FWE}	T	Z	MNI_{XYZ}	Nearest Gray Matter
0.97	0.79	19	0.99	4.72	3.72	24 54 -10	Right Middle frontal gyrus
0.99	0.79	15	0.23	4.40	3.54	40 8 4	Right middle/anterior insula
1.00	0.79	10	0.33	4.21	3.43	12 20 46	Right dorsal anterior cingulate
1.00	0.79	11	0.31	4.12	3.38	28 34 -22	Right inferior frontal gyrus
0.99	0.79	12	0.29	3.81	3.20	2 20 54	Right superior frontal gyrus

Negative PPI's

Cluster			Peak				
P_{FWE}	P_{FDR}	Size	P_{FWE}	T	Z	MNI_{XYZ}	Nearest Gray Matter
0.29	0.049	72	0.96	4.91	3.82	64 -10 26	Right precentral gyrus
				3.85	3.22	66 -6 36	Right precentral gyrus
0.99	0.33	15	0.96	4.58	3.64	2 36 -18	Right medial frontal gyrus
0.99	0.33	10	1.00	4.24	3.45	40 -60 32	Right parietal angular gyrus

Right amygdala seed

Positive PPI's

Cluster			Peak				
P_{FWE}	P_{FDR}	Size	P_{FWE}	T	Z	MNI_{XYZ}	Nearest Gray Matter
0.98	0.69	14	0.83	5.20	3.97	36 -32 22	Right posterior insula
0.94	0.69	19	0.97	4.75	3.74	36 12 24	White matter

There were no significant negative PPI's for the right amygdala seed.

Supplemental References

1. Friston KJ, Buechel C, Fink GR, Morris J, Rolls E, Dolan RJ. Psychophysiological and modulatory interactions in neuroimaging. Neuroimage. 1997;6(3):218-29.

2. Gitelman DR, Penny WD, Ashburner J, Friston KJ. Modeling regional and psychophysiologic interactions in fMRI: the importance of hemodynamic deconvolution. Neuroimage. 2003;19(1):200-7.

3. Roy AK, Shehzad Z, Margulies DS, Kelly AM, Uddin LQ, Gotimer K, Biswal BB, Castellanos FX, Milham MP. Functional connectivity of the human amygdala using resting state fMRI. NeuroImage. 2009;45(2):614-26.